3072 *Chem. Mater.* **2009**, *21*, 3072–3078
DOI:10.1021/cm803297q

CHEMISTRY OF MATERIALS
Article

Crystal Growth, Structure, and Physical Properties of $Ln(Cu,Ga)_{13-x}$ (Ln = La−Nd, Eu; $x \approx 0.2$)

Jung Young Cho,[†] Evan L. Thomas,[§] Yusuke Nambu,[⊥] Cigdem Capan,[‡] Amar B Karki,[‡] David P. Young,[‡] Kentarou Kuga,[⊥] Satoru Nakatsuji,[⊥] and Julia Y. Chan*,[†]

[†]*Department of Chemistry and* [‡]*Department of Physics and Astronomy, Louisiana State University, Baton Rouge, Louisiana 70803,* [§]*National Institute of Standards and Technology, Materials Science and Engineering Laboratory, Gaithersburg, Maryland 20899, and* [⊥]*Institute for Solid State Physics, University of Tokyo, Kashiwa 277-8581, Japan*

Received December 6, 2008. Revised Manuscript Received June 9, 2009

Single crystals of $Ln(Cu,Ga)_{13-x}$ (Ln = La−Nd, Eu; $x \approx 0.2$) were grown using Ga flux and their structures determined by single-crystal X-ray diffraction. The $Ln(Cu,Ga)_{13-x}$ (Ln = La−Nd, Eu; $x \approx 0.2$), adopting $NaZn_{13}$ structure type, crystallizes in the cubic $Fm\overline{3}c$ (No. 226) space group, with $Z = 8$ and lattice parameters $a \approx 11.8$ Å. Magnetic susceptibility and heat capacity measurements do not show any indication of long-range magnetic ordering down to 2 K for magnetic analogues. Metallic behavior is observed in the range of 2−300 K for each compound. A large positive magnetoresistance up to 154% at a field (μ_0H) of 9 T is also observed for $Pr(Cu,Ga)_{12.85(1)}$. Most interestingly, the Pr analogue shows T^2 temperature-dependent resistivity and satisfies Kadowaki-Woods relation, which is indicative of heavy-fermion behavior. Here, we present the crystal structures and physical properties of $Ln(Cu,Ga)_{13-x}$ (Ln = La−Nd, Eu; $x \approx 0.2$).

Introduction

Intermetallic compounds adopting $NaZn_{13}$-type have been of great interest due to highly correlated electron systems such as heavy-fermion behavior, which shows enhanced electronic masses ($m^* \geq 100\ m_e$) and superconductivity at low temperatures.[1,2] UBe_{13} has been reported as a heavy-fermion compound with the electronic specific-heat coefficient $\gamma \approx 1100$ mJ mol^{-1} K^{-2} and shows an unconventional superconducting state mediated by *f*-electrons below 0.85 K,[3−8] and an enhanced $\gamma \approx 58$ mJ mol^{-1} K^{-2} has been shown in $CeBe_{13}$ which is a mixed-valence system.[6,9,10] Correlated electronic phenomena due to the 4f or 5f moments on the $CeBe_{13}$ and UBe_{13} compounds are primarily due to its simple cubic symmetry.

Heavy-fermion behavior is associated with the valence instability of the 4f electrons in Ce-, U-, or Yb-based compounds.[11−14] However, until recently, only several Pr-based heavy-fermion compounds have been reported. Heavy-fermion behavior in Pr-based intermetallic compounds is quite exotic because it is well-known that the localized 4f^2-electrons of Pr^{3+} ions are stable. The Heusler-type $PrInAg_2$ ($\gamma \approx 6500$ mJ mol^{-1} K^{-2}) has been reported as the first Pr-based heavy-fermion compound and its resistivity is not quadratic in T.[15−18] In contrast to $PrInAg_2$, $PrFe_4P_{12}$ shows T^2 temperature-dependent resistivity due to the Fermi liquid behavior in the heavy-fermion state with $\gamma \approx 1400$ mJ mol^{-1} K^{-2} in the applied field of $\mu_0H = 6$ T, satisfying the Kadowaki−Woods

*To whom correspondence should be addressed. E-mail: jchan@lsu.edu. Phone: (225) 578-2695. Fax: (225) 578-3458.

(1) Fisk, Z.; Sarrao, J. L.; Thompson, J. D. *Curr. Opin. Solid State Mater. Sci.* **1996**, *1*, 42–46.
(2) Fisk, Z.; Sarrao, J. L.; Smith, J. L.; Thompson, J. D. *Proc. Natl. Acad. Sci. U.S.A.* **1995**, *92*, 6663–6667.
(3) Ott, H. R.; Rudigier, H.; Fisk, Z.; Smith, J. L. *Phys. Rev. Lett.* **1983**, *50*, 1595–1598.
(4) Smith, J. L.; Fisk, Z.; Willis, J. O.; Batlogg, B.; Ott, H. R. *J. Appl. Phys.* **1984**, *55*, 1996–2000.
(5) Maple, M. B.; Chen, J. W.; Lambert, S. E.; Fisk, Z.; Smith, J. L.; Ott, H. R.; Brooks, J. S.; Naughton, M. J. *Phys. Rev. Lett.* **1985**, *54*, 477–480.
(6) Cox, D. L. *Phys. Rev. B: Condens. Matter* **1987**, *35*, 6504–6516.
(7) Reinders, P. H. P.; Wand, B.; Steglich, F.; Fraunberger, G.; Stewart, G. R.; Andrian, G. *Europhys. Lett.* **1994**, *25*, 619–624.
(8) Kim, J. S.; Stewart, G. R. *Phys. Rev. B: Condens. Matter* **1995**, *51*, 16190–16193.
(9) Wilson, Z. S.; Macaluso, R. T.; Bauer, E. D.; Smith, J. L.; Thompson, J. D.; Fisk, Z.; Stanley, G. G.; Chan, J. Y. *J. Am. Chem. Soc.* **2004**, *126*, 13926–13927.
(10) Besnus, M. J.; Kappler, J. P.; Meyer, A. *Solid State Commun.* **1983**, *48*, 835–838.
(11) Fisk, Z.; Sarrao, J. L.; Smith, J. L.; Thompson, J. D. *Proc. Natl. Acad. Sci. U.S.A.* **1995**, *92*, 6663–6667.
(12) Holmes, A. T.; Jaccard, D.; Miyake, K. *J. Phys. Soc. Jpn.* **2007**, *76*, 051002/1–051002/10.
(13) Steglich, F. *J. Phys. Soc. Jpn.* **2005**, *74*, 167–177.
(14) Miyake, K.; Narikiyo, O.; Onishi, Y. *Physica B* **1999**, *259−261*, 676–677.
(15) Yatskar, A.; Beyermann, W. P.; Movshovich, R.; Canfield, P. C. *Phys. Rev. Lett.* **1996**, *77*, 3637–3640.
(16) Yatskar, A.; Beyermann, W. P.; Movshovich, R.; Canfield, P. C.; Panchula, A.; Bud'ko, S. L. *Physica B* **1997**, *230−232*, 46–48.
(17) Mitamura, H.; Takeshita, N.; Uwatoko, Y.; Mori, H.; Yamaguchi, A.; Tomita, T.; Wada, H.; Mori, N.; Ishimoto, H.; Goto, T. *Physica B* **2000**, *281&282*, 150–151.
(18) Matsuda, T. D.; Okada, H.; Sugawara, H.; Aoki, Y.; Sato, H.; Andreev, A. V.; Shiokawa, Y.; Sechovsky, V.; Honma, T.; Yamamoto, E.; Onuki, Y. *Physica B* **2000**, *281&282*, 220–222.

 Published on Web 07/01/2009

relation (A/γ^2).[18−22] The first Pr-based heavy-fermion superconductor, $PrOs_4Sb_{12}$, orders at $T_c = 1.85$ K with $\gamma \approx 350$ mJ mol^{-1} K^{-2}.[23−26]

On the exploration of the *Ln*−Cu-Ga system, the Sm_2NiGa_{12}-type[27] structure can be stabilized via flux growth for early lanthanides in the Ga rich region with reaction ratios of 1.5:1:15 and 2:1:20.[28] Ce_2CuGa_{12} is paramagnetic down to 2 K with an enhanced $\gamma \approx 67$ mJ mol^{-1} K^{-2}.[28] When Cu concentration is increased, the *Ln*(Cu,Ga)$_{13}$-type can be synthesized for early lanthanides in *Ln*−Cu−Ga system. In this manuscript, we report the structure, magnetism, resistivity, and heat capacity of *Ln*(Cu,Ga)$_{13-x}$ (*Ln* = La−Nd, Eu; $x \approx 0.2$). We also report the observation of heavy-fermion behavior in the compound Pr(Cu,Ga)$_{12.85(1)}$.

Experimental Section

Synthesis. Single crystals of *Ln*(Cu,Ga)$_{13-x}$ (*Ln* = La−Nd, Eu; $x \approx 0.2$) were successfully grown in excess Ga flux. *Ln* (*Ln* = La−Nd, Eu; chunks, 99.9%, Alfa Aesar), Cu (powder, 99.999%, Alfa Aesar), and Ga (pellets, 99.9999%, Alfa Aesar) with a total weight of ca. 2.5 g were mixed in the ratio *Ln*:Cu:Ga = 1:5:20 and placed into an alumina crucible. The crucible and mixture were then sealed under vacuum in a fused silica tube and heated to 1373 K for 7 h. The tube was slowly cooled to 673 K at a rate of 10 K/h, before removing from the furnace. The excess molten flux was then removed from the silvery cubic crystals (Figure 1) by centrifugation, and the crystals were stable in air. A diluted HCl (1 M) solution was used to remove the remaining Ga flux on the surfaces of crystals. After the crystals were etched for several hours, their silvery surfaces turned a reddish color, which indicates the reduction of Cu and the completion of removal of Ga flux on crystal surfaces. The reduced Cu was successfully removed by using a diluted HNO_3 (30%) solution. Our goal for this study is not to do a full phase diagram analysis, but rather highlight the composition that is relevant to our studies. We are able to synthesize the compounds adopting the $NaZn_{13}$ structure type from all reaction ratios between 1:3:20 and 1:11:20 via flux growth. For the 1:2:20 ratio, we stabilized compounds of the $ThCr_2Si_2$ structure type. In our paper, we discuss compounds from the reaction of 1:5:20 to give a consistent condition for physical properties for the series.

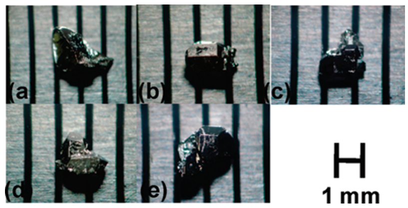

Figure 1. Single crystals of *Ln*(Cu,Ga)$_{13-x}$ (*Ln* = La−Nd, Eu; $x \approx 0.2$) are shown. (a−(e) correspond to the order for La−Nd, and Eu, respectively.

Single-Crystal X-ray Diffraction and Elemental Analysis. Crystal fragments $\approx 0.03 \times 0.03 \times 0.03$ mm^3 of *Ln*(Cu,Ga)$_{13-x}$ (*Ln* = La−Nd, Eu; $x \approx 0.2$) were mounted onto a glass fiber using epoxy. Intensity data were collected on a Bruker Nonius KappaCCD single-crystal diffractometer equipped with Mo Kα radiation (λ = 0.71073 Å) up to $\theta = 30.0°$ at 298 K by using Nonius SuperGUI software. Data reduction and integration were performed with the maXus package. Direct methods were used to solve the structure. SHELXL97 was used to refine the structural model of the *Ln*(Cu,Ga)$_{13-x}$ (*Ln* = La−Nd, Eu; $x \approx 0.2$) compounds, and data were corrected with extinction coefficients and refined with anisotropic displacement parameters. Initial refinement with a fully occupied formula yielded relatively large displacement parameters of the 8*b* sites. This led to the refinement of the occupancy of all crystallographic sites by freeing the site occupancy factor in separate sequences of least-squares cycles. The occupancy of the 8*b* site was refined to be 79.3(8)−86.3(8)%, while the other sites refined to values near unity. Final refinement with a partial occupancy for the 8*b* site converged with very small final difference residual peaks and well-behaved displacement parameters. Similar partial occupancies on the 8*b* sites have been reported in the isostructural compounds $EuZn_{13-x}$ and AZn_{13} (*A* = Ca, Sr, Ba).[29,30] Further crystallographic parameters for *Ln*(Cu,Ga)$_{13-x}$ (*Ln* = La−Nd, Eu; $x \approx 0.2$) are provided in Table 1. Atomic positions and displacement parameters for *Ln*(Cu,Ga)$_{13-x}$ (*Ln* = La−Nd, Eu; $x \approx 0.2$) are provided in Table 2, and selected interatomic distances are presented in Table 3. Single crystals of *Ln*(Cu, Ga)$_{13-x}$ (*Ln* = La−Nd, Eu; $x \approx 0.2$) were analyzed with a JEOL JSM-5060 scanning electron microscope equipped with an energy-dispersive spectrometer. The accelerating voltage was 15 kV with beam to sample distance of 20 mm. An average 5−7 scans were performed on each single crystal. Elemental analysis of the composition of the crystals was also performed using optical emission spectroscopy (ICP-OES) for all analogues (La, Ce, Pr, Nd, Eu). The compositions obtained for each analogue are as follows: La(Cu,Ga)$_{12.50(15)}$, Ce(Cu,Ga)$_{12.90(11)}$, Pr(Cu, Ga)$_{13.30(29)}$, Nd(Cu,Ga)$_{12.91(30)}$, Eu(Cu,Ga)$_{12.32(10)}$. The compositions are within the limits as obtained from single-crystal X-ray diffraction with the sum of Cu and Ga concentration ~12.8. The compositions are summarized in Table 4. For the purpose of discussion of physical properties, these compounds are represented as *Ln*(Cu,Ga)$_{13}$.

Physical Property Measurements. Magnetization data were obtained using a Quantum Design SQUID magnetometer. The temperature-dependent magnetization data were obtained under field-cooled conditions from 2 to 300 K with an applied field ($\mu_0 H$) of 0.1 T. Field-dependent measurements were collected at

(19) Sugawara, H.; Matsuda, T. D.; Abe, K.; Aoki, Y.; Sato, H.; Nojiri, S.; Inada, Y.; Settai, R.; Onuki, Y. *J. Magn. Magn. Mater.* **2001**, *226−230*, 48–50.
(20) Aoki, Y.; Namiki, T.; Matsuda, T. D.; Sugawara, H.; Sato, H. *Physica B* **2002**, *312&313*, 823–824.
(21) Kadowaki, K.; Woods, S. B. *Solid State Commun.* **1986**, *58*, 507–509.
(22) Miyake, K.; Matsuura, T.; Varma, C. M. *Solid State Commun.* **1989**, *71*, 1149–1153.
(23) Bauer, E. D.; Frederick, N. A.; Ho, P. C.; Zapf, V. S.; Maple, M. B. *Phys. Rev. B: Condens. Matter* **2002**, *65*, 100506/1–100506/4.
(24) Sugawara, H.; Osaki, S.; Saha, S. R.; Aoki, Y.; Sato, H.; Inada, Y.; Shishido, H.; Settai, R.; Onuki, Y.; Harima, H.; Oikawa, K. *Phys. Rev. B: Condens. Matter* **2002**, *66*, 220504/1–220504/4.
(25) Aoki, Y.; Tsuchiya, A.; Kanayama, T.; Saha, S. R.; Sugawara, H.; Sato, H.; Higemoto, W.; Koda, A.; Ohishi, K.; Nishiyama, K.; Kadono, R. *Phys. Rev. Lett.* **2003**, *91*, 067003/1–067003/4.
(26) Izawa, K.; Nakajima, Y.; Goryo, J.; Matsuda, Y.; Osaki, S.; Sugawara, H.; Sato, H.; Thalmeier, P.; Maki, K. *Phys. Rev. Lett.* **2003**, *90*, 117001/1–117001/4.
(27) Chen, X. Z.; Small, P.; Sportouch, S.; Zhuravleva, M.; Brazis, P.; Kannewurf, C. R.; Kanatzidis, M. G. *Chem. Mater.* **2000**, *12*, 2520–2522.
(28) Cho, J. Y.; Millican, J. N.; Moldovan, M.; Young, D. P.; Sokolov, D.; Aronson, M. C.; Chan, J. Y. *Chem. Mater.* **2008**, *20*, 6116−6123.
(29) Wendorff, M.; Roehr, C. *J. Alloys Compd.* **2006**, *421*, 24–34.
(30) Saparov, B.; Bobev, S. *J. Alloys Compd.* **2008**, *463*, 119–123.

Table 1. Crystallographic Data

			Crystal Data		
compd	$La(Cu,Ga)_{12.83(1)}$	$Ce(Cu,Ga)_{12.84(1)}$	$Pr(Cu,Ga)_{12.85(1)}$	$Nd(Cu,Ga)_{12.86(1)}$	$Eu(Cu,Ga)_{12.79(1)}$
[a]composition	$La(Cu,Ga)_{12.50(15)}$	$Ce(Cu,Ga)_{12.90(11)}$	$Pr(Cu,Ga)_{13.30(29)}$	$Nd(Cu,Ga)_{12.91(30)}$	$Eu(Cu,Ga)_{12.32(10)}$
a (Å)	11.849(5)	11.824(4)	11.811(5)	11.803(4)	11.896(6)
V (Å^3)	1663.6(12)	1653.1(10)	1647.6(12)	1644.3(10)	1683.5(15)
Z	8	8	8	8	8
cryst dimension (mm^3)	0.03×0.03× 0.03	0.05×0.05×0.05	0.03×0.03×0.03	0.03×0.03×0.03	0.05×0.05×0.05
cryst syst	cubic	cubic	cubic	cubic	cubic
space group	$Fm\bar{3}c$	$Fm\bar{3}c$	$Fm\bar{3}c$	$Fm\bar{3}c$	$Fm\bar{3}c$
θ range (deg)	3.44−29.88	3.45−29.95	3.45−29.99	3.45−29.95	3.43−29.99
μ (mm^{-1})	39.941	41.015	41.383	43.148	41.636
			Data Collection		
no. of measured reflns	346	322	319	338	286
no. of independent reflns	123	123	123	120	123
reflns with $I > 2\sigma(I)$	119	121	118	117	119
R_{int}	0.0231	0.0401	0.0318	0.0204	0.0292
h	−16→16	−16→16	−16→16	−16→16	−16→16
k	−10→10	−10→10	−10→10	−10→10	−10→10
l	−10→10	−10→10	−10→10	−10→10	−10→10
			Refinement		
$R_1[F^2 > 2\sigma(F^2)]$[b]	0.0213	0.0233	0.0252	0.0159	0.0247
$wR_2(F^2)$[c]	0.0452	0.0516	0.0585	0.0331	0.0472
no. of reflns	123	123	123	120	123
no. of params	12	12	12	12	12
$\Delta\rho_{max}$ (e Å^{-3})	1.268	1.571	1.379	1.039	1.978
$\Delta\rho_{min}$ (e Å^{-3})	−0.922	−1.407	−1.073	−0.716	−1.070

[a] Composition from elemental analysis. [b] $R_1=\Sigma||F_o| - |F_c||/\Sigma|F_o|$. [c] $wR_2=[\Sigma[w(F_o^2 - F_c^2)^2]/\Sigma[w(F_o^2)^2]]^{1/2}$. $w=1/[\sigma^2(F_o^2) + (0.0152P)^2 + 0.0000P]$, $w=1/[\sigma^2(F_o^2) + (0.0219P)^2 + 1.8765P]$, $w=1/[\sigma^2(F_o^2) + (0.0186P)^2 + 27.6561P]$, $w=1/[\sigma^2(F_o^2) + (0.0000P)^2 + 14.6592P]$, $w=1/[\sigma^2(F_o^2) + (0.0107P)^2 + 0.0000P]$, for La, Ce, Pr, Nd, and Eu compound, respectively.

Table 2. Atomic Positions and Atomic Displacement

atom	Wyckoff position	x	y	z	occupancy	U_{eq} (Å^2)[a]
La	8a	1/4	1/4	1/4	1	0.0074(3)
Cu	8b	0	0	0	0.831(9)	0.0094(6)
M[b]	96i	0	0.17791(4)	0.12139(4)	1	0.0102(4)
Ce	8a	1/4	1/4	1/4	1	0.0033(3)
Cu	8b	0	0	0	0.836(9)	0.0047(6)
M[b]	96i	0	0.17797(4)	0.12153(4)	1	0.0064(4)
Pr	8a	1/4	1/4	1/4	1	0.0048(4)
Cu	8b	0	0	0	0.853(13)	0.0062(9)
M[b]	96i	0	0.17823(6)	0.12164(6)	1	0.0071(5)
Nd	8a	1/4	1/4	1/4	1	0.0092(3)
Cu	8b	0	0	0	0.863(8)	0.0100(6)
M[b]	96i	0	0.17832(4)	0.12165(4)	1	0.0120(3)
Eu	8a	1/4	1/4	1/4	1	0.0100(3)
Cu	8b	0	0	0	0.793(8)	0.0108(7)
M[b]	96i	0	0.17804(4)	0.12107(4)	1	0.0122(4)

[a] U_{eq} is defined as one-third of the trace of the orthogonalized U_{ij} tensor. [b] M = Cu or Ga.

3 K for fields ($\mu_0 H$) between 0 and 5 T then swept from 5 T back to 0 T. The electrical resistivity data were measured by the standard four-probe AC technique using a Quantum Design Physical Property Measurement System.

Results and Discussion

Structure. $Ln(Cu,Ga)_{13}$ (Ln = La−Nd, Eu), adopting the $NaZn_{13}$ structure type, crystallize in the cubic $Fm\bar{3}c$ (No. 226) space group with Ln, Cu, M (M = Cu or Ga) occupying 8a, 8b, and 96i, respectively. Figure 2a shows the Cu-centered M (M = Cu or Ga) icosahedra and Ce atoms occupying the cavities between icosahedra of Ce$(Cu,Ga)_{12.84(1)}$. However, this description might overlook the interatomic distances between icosahedra, 2.463(1)−2.652(1) Å, which are close to the ones within the icosahedron. Therefore, this structure can be viewed with interconnections between icosahedra as shown in Figure 2b. These networks have been described as stellae quadrangulae (tetracapped tetrahedra).[31] The Ce atom in the 8a Wyckoff site is coordinated by 24 neighbor atoms, which is known as snub cube. Three different representations of polyhedra such as the Ce-centered snub cube, Cu-centered icosahedra, and the stellae quadrangula are shown in Figure 3a−c.

Although Cu and Ga are not distinguishable by X-ray diffraction, our refined model seems to be most

(31) Nyman, H.; Andersson, S. *Acta Crystallogr., Sect. A* **1979**, *35*, 934–937.

Table 3. Selected Interatomic Distances (Å)

atoms[a]	$La(Cu,Ga)_{12.83(1)}$	$Ce(Cu,Ga)_{12.84(1)}$	$Pr(Cu,Ga)_{12.85(1)}$	$Nd(Cu,Ga)_{12.86(1)}$	$Eu(Cu,Ga)_{12.79(1)}$
Ln−*M*	3.4390(15)	3.4309(12)	3.4258(15)	3.4231(12)	3.4540(18)
Cu−*M*	2.5521(12)	2.5481(10)	2.5486(13)	2.5477(10)	2.5613(14)
M−*M*	2.4705(12)	2.4628(10)	2.4565(15)	2.4540(11)	2.4840(14)
M−*M*	2.6385(12)	2.6341(10)	2.6348(14)	2.6341(10)	2.6494(14)

[a] *M* = Cu or Ga.

Table 4. Composition as Obtained from Electron Probe Microanalysis and ICP-OES

refined composition	analysis method	Cu	Ga	Sum
$La(Cu,Ga)_{12.83(1)}$	EDS	6.60	5.90	12.50(15)
	ICP-OES	6.22(6)	6.09(6)	12.31
$Ce(Cu,Ga)_{12.84(1)}$	EDS	6.83	6.06	12.90(11)
	ICP-OES	6.15(6)	6.29(6)	12.44
$Pr(Cu,Ga)_{12.85(1)}$	EDS	7.01	6.28	13.30(29)
	ICP-OES	7.21(1)	7.62(1)	14.83
$Nd(Cu,Ga)_{12.86(1)}$	EDS	6.78	6.12	12.91(30)
	ICP-OES	6.04(6)	5.85(6)	11.89
$Eu(Cu,Ga)_{12.79(1)}$	EDS	6.54	6.75	13.29(73)
	ICP-OES	5.90(1)	6.42(1)	12.32

stabilized when Cu is occupying the 8*b* site ($m\overline{3}$, center of the icosahedra) in these compounds. This is also observed in the $BaCu_5Al_8$ and $EuCu_{6.5}Al_{6.5}$ compounds, which show the three-dimensional $[Cu_xAl_{13-x}]$ network having mostly Cu atoms residing in the 8*b* site.[32] The systematic study of the compositional variation and theoretical calculations in $BaCu_xAl_{13-x}$ suggest that the $NaZn_{13}$ structure type forms within a narrow range of the *x* between 5 and 6.[32] Based on rigid-band calculations, Nordell and Miller show that optimal intraicosahedral bonding on $BaCu_xAl_{13-x}$ has 40.5 electrons per formula unit, which corresponds to simple electron counting by treating the valence *s*, *p*, and *d* electrons of the element at the 8*b* site, while counting only the valence *s* and *p* electrons of the elements at the 8*a* and 96*i* sites.[32]

Valence electron counting rules assume that the anionic cluster, which was proposed and consistent based on previous analysis of Nordell and Miller. As suggested by Bobev et al.,[30] geometric and electronic factors have to be considered simultaneously. For the $Ln(Cu,Ga)_{13}$ compounds, the (Cu,Ga)-deficiency as determined from single crystal X-ray diffraction is consistent with the previously reported $EuZn_{12.8}$ where the valence electron concentration is within the valence electron count from previous $AEZn_{13-x}$ studies (AE = alkaline earth metals). Our elemental analysis of the $Ln(Cu,Ga)_{13}$ (*Ln* = La−Nd, Eu) compounds shows a slightly higher Cu concentration than Nordell and Miller's compounds. Although our lanthanide compounds are isostructural to $EuZn_{12.8}$, determining valence electron may not be applicable to $Ln(Cu,Ga)_{13}$ compounds but rather, the stability of the lanthanide phases is attributed to the size of the lanthanide and the coloring effect.

Figure 4 shows the unit-cell volume of $Ln(Cu,Ga)_{13}$ (*Ln* = La−Nd, Eu) as a function of lanthanide. A decrease in the unit-cell volume and the corresponding decrease in lattice parameters follows the lanthanide contraction except $Eu(Cu,Ga)_{12.79(1)}$, which shows a deviation in the unit-cell volume. This deviation is consistent with the divalent oxidation state of Eu analogue. From our study of *Ln*−Cu−Ga system, we have observed that early lanthanides (La−Nd, Eu) adopt the $NaZn_{13}$ structure type and late lanthanides adopt the $ThMn_{12}$ structure type.[33]

Physical Properties. The temperature-dependent magnetic susceptibility of $Ln(Cu,Ga)_{13}$ (*Ln* = Ce−Nd, Eu) at an external field ($\mu_0 H$) of 0.1 T is shown in Figure 5. No long-range magnetic ordering is observed down to 2 K for all compounds. The magnetic susceptibility data of $Ln(Cu,Ga)_{13}$ (*Ln* = Ce−Nd, Eu) were fitted to a modified Curie−Weiss law in the following form: $\chi(T) = \chi_0 + C/(T - \theta)$, where χ_0 denotes the temperature-independent term, C represents the Curie constant, and θ is the Weiss temperature. The effective moments of 2.36 μ_B/Ce, 3.32 μ_B/Pr, and 3.40 μ_B/Nd are close to the calculated values for Ce^{3+}, Pr^{3+}, and Nd^{3+}, respectively. The negative Weiss temperatures of −3.83 (Ce), − 1.27 (Pr), and − 1.80 (Nd) are indicative of antiferromagnetic correlations in these compounds. The effective moment of 8.06 μ_B/Eu with θ = 1.85 in the Eu analogue indicates that Eu ion is in the divalent state with an f^7 electronic configuration. This is consistent with the deviation observed in the cell volume as a function of lanthanides. The positive sign of the Weiss temperature for Eu analogue is indicative of ferromagnetic coupling in contrast to the three other analogues. The small Weiss temperatures for all compounds suggest that the lanthanide moments are very weakly coupled in this system, which is consistent with the large *Ln*−*Ln* separation of ≈ 5.9 Å. A summary of the magnetic properties of $Ln(Cu,Ga)_{13}$ (*Ln* = Ce−Nd, Eu) is shown in Table 5.

Figure 6 shows the field-dependent isothermal magnetization of $Ln(Cu,Ga)_{13}$ (*Ln* = Ce−Nd, Eu) measured at constant temperature of 3 K. The magnetization at 5 T is only about 0.89 μ_B, 1.42 μ_B, and 1.51 μ_B for Ce, Pr, and Nd analogue, respectively, which is much smaller than the calculated value of 2.14 μ_B, 3.20 μ_B, and 3.27 μ_B for each Ln^{3+} ion and is probably due to the crystal field splitting of Ln^{3+} in its cubic environment. This result suggests a local moment for these ions is not linear but shows a saturating behavior. However, for Eu compound the magnetization saturates at 5 T with a value of 6.85 μ_B close to the expected value of 7.0 μ_B for Eu^{2+} ion.

(32) Nordell, K. J.; Miller, G. J. *Inorg. Chem.* **1999**, *38*, 579–590.

(33) Drake, B. L.; Cho, J. Y.; Capan, C.; Kuga, K.; Karki, A. B.; Nambu, Y.; Nakatsuji, S.; Young, D. P.; Chan, J. Y. To be submitted.

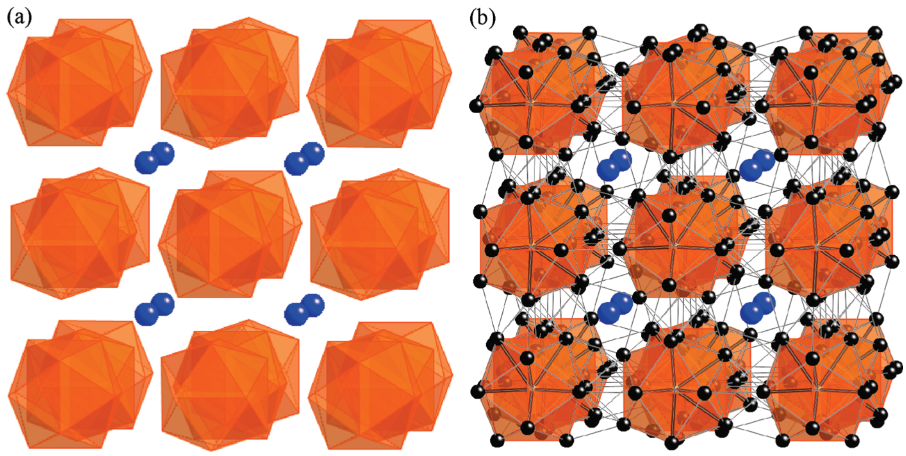

Figure 2. (a) Crystal structure of $Ce(Cu,Ga)_{12.84(1)}$ is shown as Cu atom-centered icosahedral packing diagram, where the Ce atoms are represented with blue spheres. (b) Structural representation in terms of stella quadrangula.

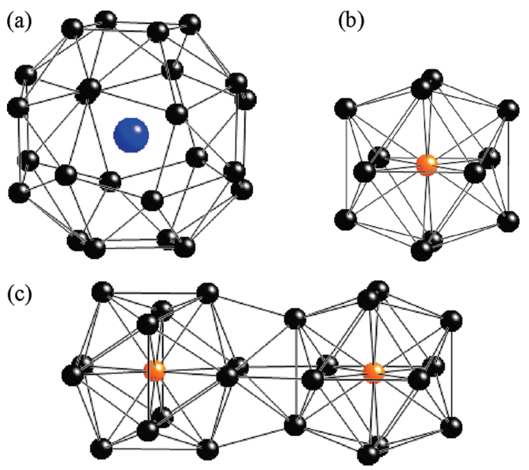

Figure 3. (a) Ce atom-centered snub cube, (b) Cu atom-centered icosahedrons, and (c) stella quadrangula.

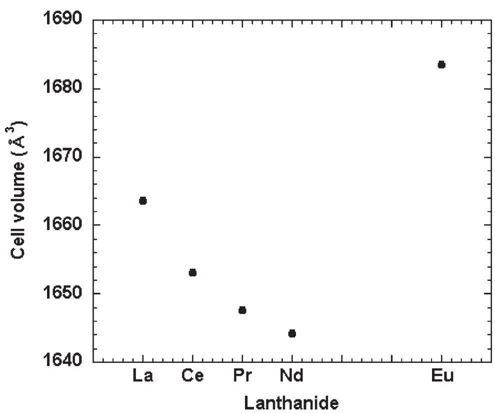

Figure 4. Unit-cell volumes as a function of lanthanide.

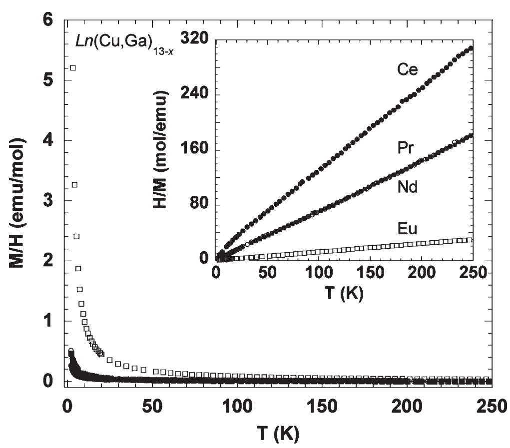

Figure 5. Magnetic susceptibility (emu/mol *Ln*) of $Ln(Cu,Ga)_{13-x}$ (Ln = Ce−Nd, Eu; $x \approx 0.2$) as a function of temperature is shown. The inset shows inverse magnetic susceptibility of $Ln(Cu,Ga)_{13-x}$ (Ln = Ce−Nd, Eu; $x \approx 0.2$).

The temperature dependence of the electrical resistivity of $Ln(Cu,Ga)_{13}$ (Ln = La−Nd, Eu), where each compound shows metallic behavior with RRR (residual resistivity ratio) values of 2.3, 1.6, 4.1, 2.4, and 1.4 for La, Ce, Pr, Nd, and Eu analogue, respectively, is shown in Figure 7. Unlike other analogues, a broad shoulder for $Pr(Cu,Ga)_{12.85(1)}$, which may indicate Kondo coherence, is observed in the resistivity below 60 K. In the inset of Figure 6, $\rho-\rho_0$ are plotted as a function of T^2 for $Pr(Cu,Ga)_{12.85(1)}$ at low temperatures, which is suggestive of a Fermi liquid behavior. The T^2 coefficient A of 0.0727 $\mu\Omega$ cm and the residual resistivity of 79.909 $\mu\Omega$ cm/K^2 were obtained by fitting the data at low temperatures ($\leq$20 K). However, other analogues do not show a linear relationship of $\rho-\rho_0$ against T^2.

Figure 8 shows the magnetoresistance (MR % = $(\rho_H-\rho_0)/\rho_0\times 100$) of single crystals of $Ln(Cu,Ga)_{13}$ (Ln = La−Nd, Eu) as a function of field (μ_0H) at 3 K. The $Ln(Cu,Ga)_{13}$ (Ln = La−Nd) compounds except Eu analogue show positive magnetoresistance, with ratios up to 23, 3, 154, and 20 at 9 T for the La, Ce, Pr, and Nd analogue, respectively. However, Eu analogue shows field-independent resistance up to 5 T, which is not shown here. Interestingly, $Pr(Cu,Ga)_{12.85(1)}$ shows much more field-dependent resistance than other analogues in this series. This large positive magnetoresistance is quite unusual because most heavy fermion system shows negative one over a wide temperature range. For instance, the heavy fermion compounds $CeCu_2Si_2$, $CeAl_3$, and UBe_{13} show the negative magnetoresistance that is predicted for

Table 5. Magnetic Properties of *Ln*(Cu,Ga)$_{13-x}$ (*Ln* = Ce−Nd, Eu; $x \approx 0.2$)

	C (emu/mol K)	θ (K)	χ_0 ($\times 10^{-4}$ cm^3/mol *Ln*)	μ_{calcd}(μ_B)	μ_{eff} (μ_B)	fit range (K)
Ce(Cu,Ga)$_{12.84(1)}$	0.70	−3.83	6.49	2.54 (Ce^{3+})	2.36	10−300
Pr(Cu,Ga)$_{12.85(1)}$	1.38	−1.27	1.92	3.58 (Pr^{3+})	3.32	10−300
Nd(Cu,Ga)$_{12.86(1)}$	1.45	−1.80	−2.84	3.62 (Nd^{3+})	3.40	10−300
Eu(Cu,Ga)$_{12.79(1)}$	8.14	1.85	4.27	7.94 (Eu^{2+})	8.06	10−260

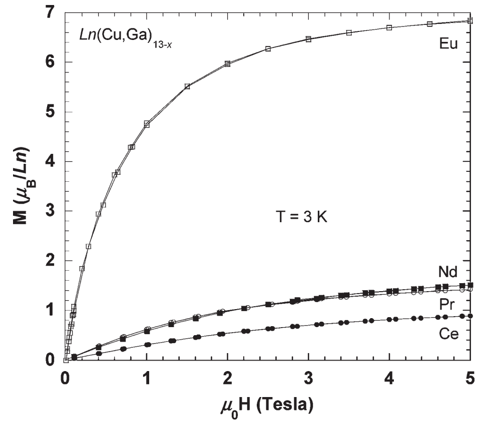

Figure 6. Magnetization of *Ln*(Cu,Ga)$_{13-x}$ (*Ln* = Ce−Nd, Eu; $x \approx 0.2$) as a function of magnetic field at 3 K.

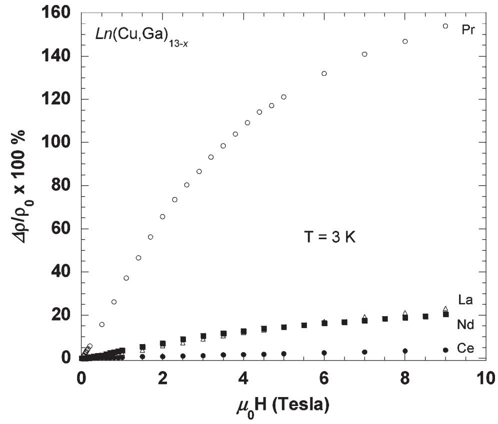

Figure 8. MR % of *Ln*(Cu,Ga)$_{13-x}$ (*Ln* = La−Nd; $x \approx 0.2$) as a function of field at 3 K is shown.

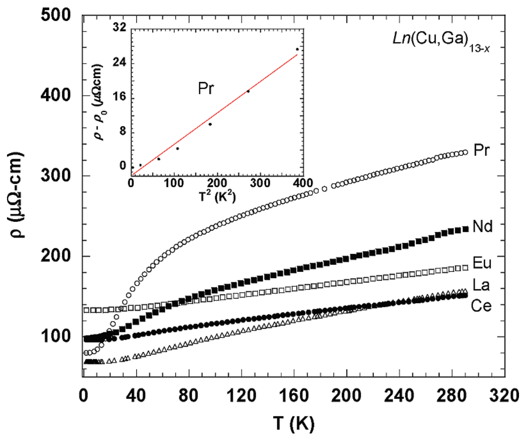

Figure 7. Normalized electrical resistivity of *Ln*(Cu,Ga)$_{13-x}$ (*Ln* = La−Nd, Eu; $x \approx 0.2$) as a function of temperature.

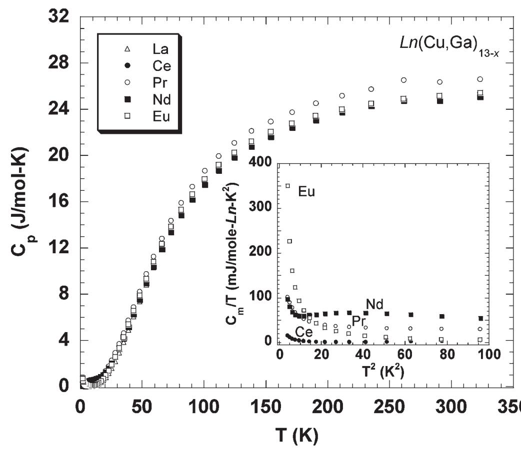

Figure 9. Specific heat of *Ln*(Cu,Ga)$_{13-x}$ (*Ln* = La−Nd; $x \approx 0.2$) as a function of temperature. The inset shows C_m/T versus T^2 for *Ln*(Cu,Ga)$_{13-x}$ (*Ln* = Ce−Nd; $x \approx 0.2$) after subtracting lattice contribution.

independent Kondo impurities.[34,35] Furthermore, the Pr-based heavy fermion system show magnetoresistance that is only about 3% at 12 T in $PrInAg_2$ at 30 mK and about 33% at 2.5 K and 4 T in $PrFe_4P_{12}$.[17,36] The fact that only the Pr analogue shows a large positive magnetoresistance suggests that its mechanism is closely related to the formation of heavy quasiparticles.

The specific heat of *Ln*(Cu,Ga)$_{13}$ (*Ln* = La−Nd) is shown in Figure 9. There is no indication of a magnetic ordering down to 2 K for *Ln*(Cu,Ga)$_{13}$ (*Ln* = Ce−Nd), consistent with their magnetic susceptibility data. As shown in the inset of Figure 9, after subtracting the phonon contribution to heat capacity $\gamma \approx 16$ mJ mol^{-1} K^{-2}, 100 mJ mol^{-1} K^{-2}, 97 mJ mol^{-1} K^{-2}, 350 mJ mol^{-1} K^{-2} are obtained for Ce, Pr, Nd, and Eu analogue, respectively, which indicates that *Ln*(Cu,Ga)$_{13}$ (*Ln* = Ce−Nd) exhibits an enhanced heavy-fermion behavior, except for the Ce analogue. With the resistivity and specific heat data of Pr(Cu,Ga)$_{12.85(1)}$ taken into account together, a Kadowaki−Woods ratio, A/γ^2, where A represents the coefficient of the quadratic term in the temperature dependence of the resistivity and γ is the coefficient of the linear term in the temperature dependence of the specific heat, of $\approx 0.727 \times 10^{-5}$ $\mu\Omega$ cm mol^2 K^2 mJ^{-2} is in the order of the expected relations for many heavy-fermion compounds.[21,37,38] As mentioned earlier, there have been only rare Pr-based heavy-fermion intermetallic compounds such as $PrInAg_2$ and the filled skutterudites PrM_4X_{12} (M = Fe, Ru, Os; X = P, As, Sb). Our

(34) Andraka, B. *Phys. Rev. B: Condens. Matter* **1995**, *52*, 16031–16033.
(35) Rauchschwalbe, U.; Steglich, F.; Rietschel, H. *Physica B* **1987**, *148*, 33–36.
(36) Sato, H.; Abe, Y.; Matsda, T. D.; Abe, K.; Namiki, T.; Sugawara, H.; Aoki, Y. *J. Magn. Magn. Mater.* **2003**, *258*, 67–72.
(37) Canfield, P. C.; Jia, S.; Mun, E. D.; Bud'ko, S. L.; Samolyuk, G. D.; Torikachvili, M. S. *Physica B* **2008**, *403*, 844–846.
(38) Torikachvili, M. S.; Jia, S.; Mun, E. D.; Hannahs, S. T.; Black, R. C.; Neils, W. K.; Martien, D.; Bud'ko, S. L.; Canfield, P. C. *Proc. Natl. Acad. Sci. U.S.A.* **2007**, *104*, 9960–9963.

preliminary interpretation on $Pr(Cu,Ga)_{12.85(1)}$ satisfying the Kadowaki−Woods ratio is similar to the case of $PrFe_4P_{12}$ which has been reported as the only $4f^2$-based Fermi liquid heavy-fermion compound.[18−20,39,40] However, further work at low temperatures is needed to establish the origin of heavy-fermion behavior on $Pr(Cu,Ga)_{12.85(1)}$ compound.

Acknowledgment. J.Y.C. acknowledges an NSF-DMR0756281 and Alfred P. Sloan Fellowship for partial support of this project. D.P.Y. acknowledges an NSF-CAREER award (DMR0449022). This work is partially supported by a Grant-in-Aid for Scientific Research (No. 21684019) from the Japanese Society for the promotion of Science and a Grant-in-Aid for Scientific Research on Innovative Areas "Heavy Electrons" (No. 20102007) of the Ministry of Education, Culture, Sports, Science and Technology, Japan. The authors thank the Materials Design and Characterization Laboratory of Institute of Solid State Physics at University of Tokyo.

(39) Aoki, Y.; Namiki, T.; Matsuda, T. D.; Abe, K.; Sugawara, H.; Sato, H. *Phys. Rev. B: Condens. Matter* **2002**, *65*, 064446/1–064446/7.
(40) Aoki, Y.; Sugawara, H.; Sato, H. *J. Alloys Compd.* **2006**, *408−412*, 21–26.